

# Growth of Horizontally Aligned Single-Walled Carbon Nanotubes on the Singular R-Plane (10–11) of Quartz

*Shohei Chiashi<sup>1</sup>, Hiroto Okabe<sup>1</sup>, Taiki Inoue<sup>1</sup>, Junichiro Shiomi<sup>1</sup>, Tadashi Sato<sup>2</sup>, Shuichi Kono<sup>2</sup>,  
Masami Terasawa<sup>2</sup> and Shigeo Maruyama<sup>1\*</sup>*

<sup>1</sup> Department of Mechanical Engineering, The University of Tokyo, 7-3-1 Hongo, Bunkyo-ku, Tokyo 113-8656, Japan

<sup>2</sup> Kyocera Kinseki Corporation, 1-8-1 Izumi-honcho, Komae, Tokyo 201-8648, Japan

maruyama@photon.t.u-tokyo.ac.jp

We used both R-cut and R-face crystal quartz substrates for the growth of horizontally aligned single-walled carbon nanotubes (SWNTs). The R-plane (10–11) is one of the low-index crystallographic planes of crystal quartz. The surface cut from a synthetic quartz block parallel to the R-plane was used as R-cut substrates, and the exposed R-plane was used as R-face substrates. We elucidated that the atomic structure of the R-plane causes the alignment of the SWNTs. While a step-and-terrace structure clearly appeared on R-face substrates, SWNTs were aligned on the terraced area of the R-plane, regardless of the direction of the step edges. Comparison between R-face and ST-cut substrates suggests that the ST-cut surface can be considered as a collection of tiny r-plane (01–11) domains, which are very similar to the R-plane (10–11).

## 1. Introduction

Single-walled carbon nanotubes (SWNTs) are promising materials for future electronic devices because they have unique electrical conductivity properties<sup>1</sup> that can be metallic or semiconducting depending on their chirality ( $n, m$ ) and high carrier mobilities<sup>2,3</sup>. Because SWNTs are stable even at high temperatures due to extremely low carbon atom diffusion, they are expected to have higher maximum current densities than copper and gold wires. However, the maximum current per SWNT is low because they have small diameters (a few nanometers). Therefore, an integration technique is required to realize SWNT-based electronic devices.

One integration method is orientation-controlled growth of SWNTs, which is generally based on chemical vapor deposition (CVD). SWNTs are aligned by applying an electric field<sup>4,5</sup>, using CVD gas flow<sup>6,7</sup>, or using single-crystal substrates<sup>8,9</sup>. Although the alignment direction can be varied by applying an electric field or gas flow, SWNTs aligned by these methods do not have very high degree of alignment. In contrast, SWNTs can be aligned in a specific direction when using single-crystal substrates with relatively high degree of alignment. Sapphire ( $\text{Al}_2\text{O}_3$ ) and quartz ( $\text{SiO}_2$ ) substrates have been used as single-crystal substrates. The alignment of SWNTs depends on the cutting angle of the substrate and the surface treatment process used, which indicates that the surface atomic structure is important for horizontally aligned SWNT growth on both sapphire<sup>8,10,11</sup> and quartz substrates<sup>9,12-16</sup>.

Horizontally aligned SWNTs have been grown on quartz substrates that have been cut at various angles (e.g., ST-, Y-, and AT-cut) and the alignment mechanism has been discussed<sup>16</sup>. It is considered that the interaction between SWNTs and the substrate surface generates a periodical potential and that SWNTs grow parallel with the potential valley. ST-cut quartz substrates are extensively used for growing horizontally aligned SWNTs. ST-cut quartz substrates are easily available because they are piezoelectric and used as stable oscillator components. However, the atomic structure of ST-cut quartz

surface is not simple and has not been determined because the cutting angle of the ST-cut does not correspond to any low-index crystallographic plane of quartz. This makes it difficult to discuss the alignment mechanism on ST-cut quartz.

To control and improve the SWNT alignment (in terms of degree of alignment, number density, etc.), it is critical to understand the surface structure of quartz substrates and the interaction between these substrates and SWNTs. In this study, we investigated the alignment mechanism on ST-cut quartz by growing SWNTs on quartz substrates with two different cutting angles, namely ST-cut and R-cut substrates. R-cut substrates are cut parallel to the singular R-plane (10–11) of quartz, which is a stable low-index surface. Moreover, we used the R-face (10–11) surface, which appears on a quartz block. We grew SWNTs on various quartz substrates. We discuss the mechanism of horizontally aligned SWNT growth based on the results obtained.

## 2. Experimental

SWNTs were synthesized by alcohol catalytic CVD<sup>17</sup>. Fe/Co nanoparticles supported on zeolite particles were used as the catalyst. Because the catalytic metal nanoparticles (Fe/Co) were supported on zeolite particles, the catalyst properties (nanoparticle size, catalyst activity, etc.) were ensured to be independent of substrates. These zeolite particles were dispersed in ethanol and the dispersion was dropped on substrates. The substrates were heated in an Ar/H<sub>2</sub> (3 vol. %) gas mixture in an electric furnace. At the CVD temperature (800 °C), the Ar/H<sub>2</sub> gas was exchanged with ethanol gas (pressure: 1 kPa; flow rate: 450 sccm) and SWNTs were synthesized. The CVD time was 10 min.

Various quartz substrates were used for supporting the zeolite particles. ST-cut and R-cut substrates (Kyocera Corp., Japan) were cut at different angles (see Fig. 1). Additionally, we used the exposed R-face (10–11) quartz substrates (Kyocera Corp., Japan). The R-face substrates were directly cut from synthetic quartz blocks. Although ST-cut quartz substrates are widely used for growing horizontally

aligned SWNTs<sup>12-16</sup>, the Miller index of ST-cut is approximately (0 23 -23 27) and the surface of ST-cut substrates does not correspond to any low-index crystallographic surface of quartz. The cutting angle of ST-cut substrates is nearly parallel to the r-plane (01-11) and that of R-cut substrates is parallel to the R-plane (0-111), which is equivalent to R-plane (10-11) (see Fig. 1). R- and r-faces are stable surfaces that appear in natural and artificially grown quartz. They have relatively low growth rates<sup>18</sup> and surfaces with similar atomic structures. In advance, mild chemical etching (30% ammonium hydrogen fluoride at 25 °C for 5 min) and annealing (at 900 °C in air for 13 h) were applied as surface treatments in some cases.

SWNTs and the quartz substrates were analyzed by scanning electron microscopy (SEM; S-4800, Hitachi) and atomic force microscopy (AFM; SPI3800N, Seiko Instrument Inc.). Raman scattering measurements were used to characterize the SWNTs. The excitation laser wavelength was 488.0 nm.

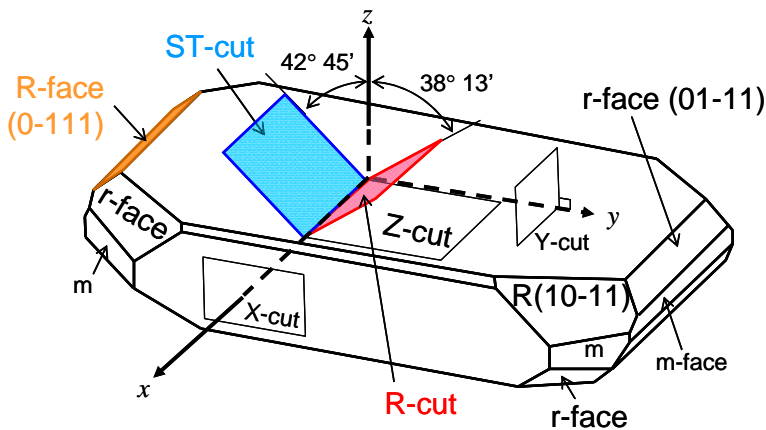


Fig. 1 Quartz block and quartz substrates with various cutting angles.

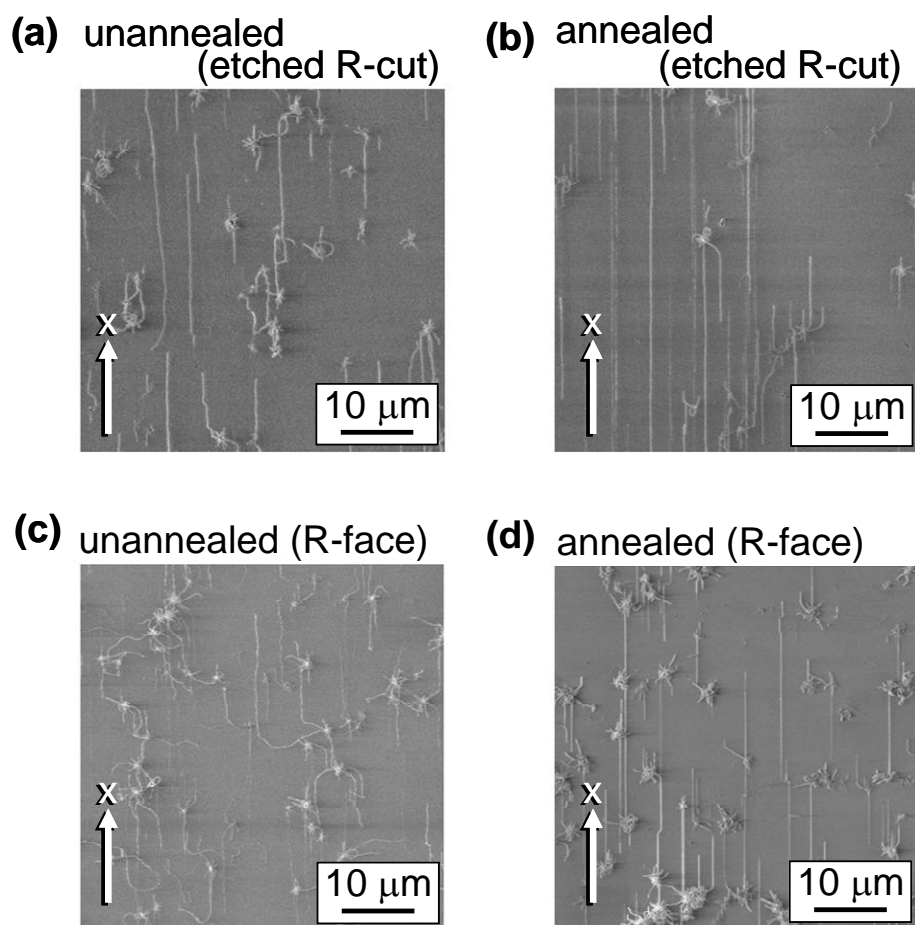


Fig. 2 SEM images of SWNTs grown on (a, b) etched R-cut and (c, d) R-face quartz substrates. The quartz substrates were (a, c) unannealed and (b, d) annealed. The arrows indicate the direction of the  $x$ -axis of crystal quartz.

### 3. Results and Discussion

Figure 2 shows SEM images of SWNTs grown on etched R-cut and R-face substrates. Substrates (b) and (d) in Fig. 2 were annealed at 900 °C for 13 h in air prior to CVD. The SEM images show zeolite particles that are a few micrometers in diameter. Many SWNTs grew from zeolite particles and some reached the surface of the quartz substrate and continued to grow, interacting with the substrates. As seen in Fig. 2, almost all the SWNTs were aligned parallel to the  $x$ -axis. Thus, horizontally aligned SWNTs were grown on etched R-cut and R-face substrates and they were aligned parallel with the  $x$ -axis. Moreover, the annealing treatment clearly enhanced the SWNT alignment. The alignment

direction and effect of annealing on etched R-cut and R-face substrates were the same as those for ST-cut substrates<sup>12,15</sup>. SWNTs were also aligned parallel to the  $x$ -axis of unetched R-cut substrates (not shown).

Figure 3 shows a Raman spectrum of SWNTs grown on quartz substrates. The distribution of radial breathing mode (RBM) peaks<sup>19</sup> in the Raman spectra indicates that the SWNT diameters range from 0.9 to 1.5 nm. The tube diameter distribution and the SWNT quality (the G- and D-band intensity ratio) were independent of the quartz substrate and annealing.

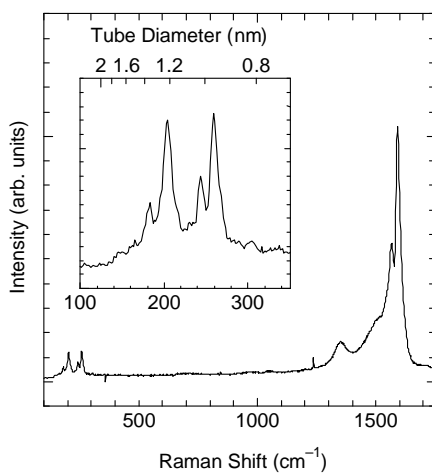


Fig. 3 Raman spectrum of SWNTs grown using a catalyst of Fe/Co nanoparticles supported on zeolite particles. Note that SWNTs were not aligned because the sample was prepared from plenty of zeolite particles on R-cut substrate for the Raman measurement. The inset shows RBM peaks in the lower wavenumber region.

Figure 4(a–c) show AFM images of an etched R-cut quartz substrate, an unetched R-cut quartz substrate, and a pristine R-face quartz substrate, respectively. For reference, Fig. 4(d) shows an AFM image of an ST-cut quartz substrate that had been chemically etched. The etched R-cut substrate (Fig. 4(a)) exhibits a complex dimpled structure, while the unetched R-cut substrate (Fig. 4(b)) has a step-and-terrace structure. The etched ST-cut substrate (Fig. 4(d)) has a dimpled structure similar to that of the etched R-cut substrate; the dimpled structure was thus considered to be caused by chemical etching.

Since the etching rate depends on the crystal plane, the surface structure of the etched quartz substrates varied depending on the cutting angle<sup>20</sup>. The step-and-terrace structure was more apparent on the R-face substrate (Fig. 4(c)). The step height was estimated to be approximately 0.3 nm from the cross-section profile (inset of Fig. 4(c)), which corresponds to the lattice spacing of the (10–11) plane (0.334 nm). This indicates that both the R-face and unetched R-cut substrate consisted of singular R-plane (10–11) and that the atomic structure of the R-plane (10–11) caused SWNTs to align parallel with the  $x$ -axis.

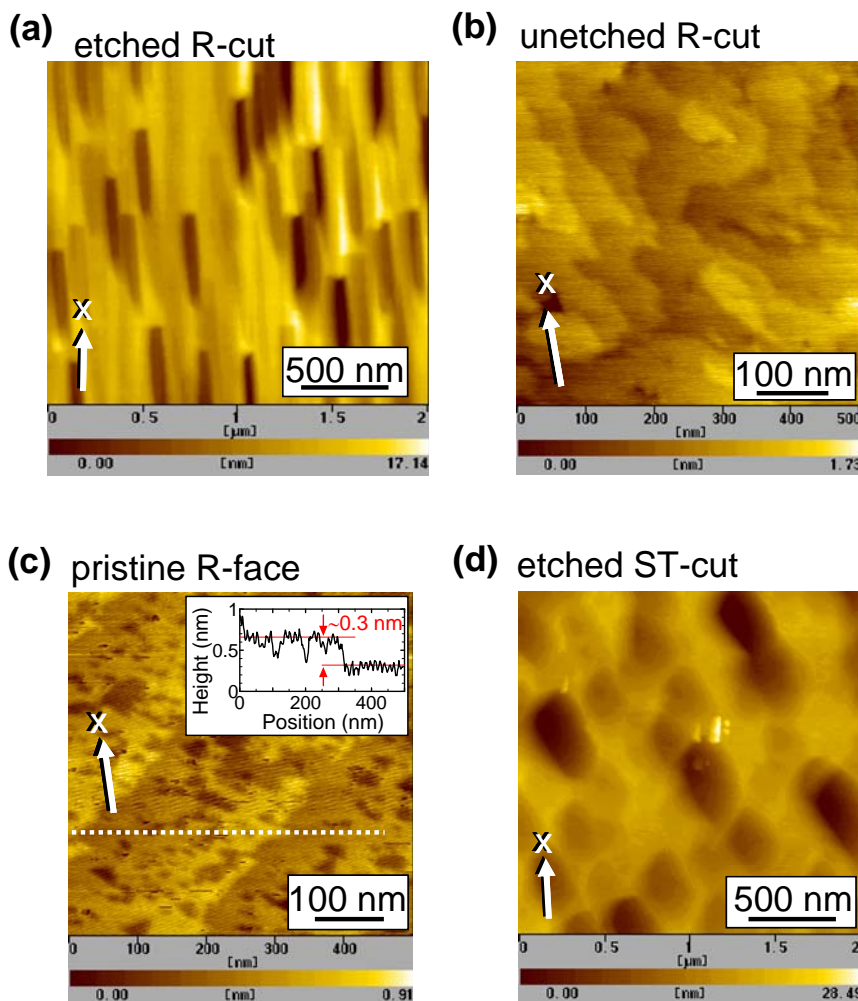


Fig. 4 AFM images of the surface structure of (a) etched R-cut, (b) unetched R-cut, (c) pristine R-face, and (d) etched ST-cut quartz substrates. These substrates are unannealed. The arrows indicate the direction of the  $x$ -axis. The inset of (c) is the cross-section profile along the dotted line.

The  $x$ -axis in quartz has high symmetry regardless of the crystal phases ( $\alpha$ -,  $\beta$ - and tridymite) and it exists on the (10–11) surface. On the other hand, the Z-cut substrate has a (0001) surface and SWNTs didn't align on it. SWNTs grown on Z-cut substrates exhibited approximately three-fold symmetry<sup>12</sup>, which corresponds to the three-fold symmetry of the atomic structure of the (0001) surface. This implies that the high translation symmetry of the atomic structure on the substrate surface directly determines the orientation of aligned SWNTs.

Crystal quartz undergoes various phase transitions on heating<sup>21</sup>. Quartz is in the  $\alpha$ -quartz phase at room temperature and transforms into  $\beta$ -quartz at 573 °C. The transition from  $\alpha$ - to  $\beta$ -quartz occurs rapidly since it involves small changes of the lattice constants. On the other hand, the phase transition between  $\beta$ -quartz and the tridymite structure at 867 °C is very slow. Although the annealing temperature (900 °C) was higher than both transition temperatures, we believe that the structure transitions didn't affect the aligned growth of SWNTs. Even though the annealing treatment clearly enhanced the SWNT alignment (see Fig. 2), AFM observations did not reveal any structural changes of R-face or unetched R-cut substrates on annealing. SWNT alignment on sapphire substrates is also enhanced by annealing<sup>22</sup> and sapphire substrates undergo structural change on annealing<sup>23</sup>. This enhanced SWNT alignment may be related to the structural change of the substrate, although the details are still under discussion<sup>24</sup>. This comparison suggests that quartz has a more stable atomic structure with respect to annealing than sapphire and annealing doesn't induce a structural change in quartz at least within the AFM resolution.

R-cut and R-face substrates showed the same SWNT alignment direction and annealing effects as ST-cut substrates. Therefore, ST-cut surface can be regarded as a collection of tiny r-plane (01–11) domains<sup>15</sup> since the angle difference between ST-cut surface and r-plane (01–11) is small (approximately 4°) and both R-plane (10–11) and r-plane (01–11) are poorly etched in general<sup>20</sup>. This suggests that SWNTs could be aligned by the domains of the r-plane (01–11) on ST-cut substrates. Although ST-cut substrates are widely used for horizontal alignment of SWNTs, their surface structure



is not atomically flat, as mentioned above. In contrast, R-cut substrates have singular R-plane (10–11) and achieve comparable or superior SWNT alignment to ST-cut substrates. Thus, R-cut substrates are suitable for growing aligned SWNTs and for investigating the SWNT alignment mechanism.

#### **4. Conclusions**

In conclusion, we synthesized horizontally aligned SWNTs on various quartz substrates (ST-cut, R-cut, and R-face) and investigated their alignment mechanism. On these quartz substrates, the SWNTs were commonly aligned parallel to the  $x$ -axis direction and the SWNT alignment was enhanced by annealing. The results showed that the atomic structure of R-plane (10–11) aligned SWNTs. Therefore, the ST-cut substrate surface is considered to be a collection of tiny r-face (01–11) domains, which align SWNTs parallel to the  $x$ -axis.

#### **Acknowledgement**

Part of this work was financially supported by Grants-in-Aid for Scientific Research (19054003, 22226006, 23760179) from the Japan Society for the Promotion of Science, and Global COE Program “Global Center of Excellence for Mechanical Systems Innovation”. T.I. was financially supported by a JSPS Research Fellowships for Young Scientists (23-8717).

#### **References**

1. Saito, R.; Dresselhaus, G.; Dresselhaus, M. S. Trigonal Warping Effect of Carbon Nanotubes. *Phys. Rev. B* **2000**, *61*, 2981-2990.
2. Fuhrer, M. S.; Kim, B. M.; Dürkop, T.; Brintlinger, T. High-Mobility Nanotube Transistor Memory. *Nano Lett.* **2002**, *2*, 755-759.

3. Dürkop, T.; Getty, S. A.; Cobas, E.; Fuhrer, M. S. Extraordinary Mobility in Semiconducting Carbon Nanotubes. *Nano Lett.* **2004**, *4*, 35-39.
4. Zhang, Y.; Chang, A.; Cao, J.; Wang, Q.; Kim, W.; Li, Y.; Morris, N.; Yenilmez, E.; Kong, J.; Dai, H. Electric-Field-Directed Growth of Aligned Single-Walled Carbon Nanotubes. *Appl. Phys. Lett.* **2001**, *79*, 3155-3157.
5. Joselevich, E.; Lieber, C. M. Vectorial Growth of Metallic and Semiconducting Single-Wall Carbon Nanotubes. *Nano Lett.* **2002**, *2*, 1137-1141.
6. Huang, S. M.; Maynor, B.; Cai, X. Y.; Liu, J. Ultralong, Well-Aligned Single-Walled Carbon Nanotube Architectures on Surfaces. *Adv. Mater.* **2003**, *15*, 1651-1655.
7. Zheng, L. X.; O'Connell, M. J.; Doorn, S. K.; Liao, X. Z.; Zhao, Y. H.; Akhadov, E. A.; Hoffbauer, M. A.; Roop, B. J.; Jia, Q. X.; Dye, R. C.; Peterson, D. E.; Huang, S. M.; Liu, J.; Zhu, Y. T. Ultralong Single-Wall Carbon Nanotubes. *Nat. Mater.* **2004**, *3*, 673-676.
8. Ismach, A.; Segev, L.; Wachtel, E.; Joselevich, E. Atomic-Step-Templated Formation of Single Wall Carbon Nanotube Patterns. *Angew. Chem., Int. Ed.* **2004**, *43*, 6140-6143.
9. Kocabas, C.; Hur, S. H.; Gaur, A.; Meitl, M. A.; Shim, M.; Rogers, J. A. Guided Growth of Large-Scale, Horizontally Aligned Arrays of Single-Walled Carbon Nanotubes and Their Use in Thin-Film Transistors. *Small* **2005**, *1*, 1110-1116.
10. Han, S.; Liu, X.; Zhou, C. Template-Free Directional Growth of Single-Walled Carbon Nanotubes on a- and r-Plane Sapphire. *J. Am. Chem. Soc.* **2005**, *127*, 5294-5295.
11. Ago, H.; Nakamura, K.; Ikeda, K.; Uehara, N.; Ishigami, N.; Tsuji, M. Aligned Growth of Isolated Single-Walled Carbon Nanotubes Programmed by Atomic Arrangement of Substrate Surface. *Chem. Phys. Lett.* **2005**, *408*, 433-438.

12. Kocabas, C.; Kang, S. J.; Ozel, T.; Shim, M.; Rogers, J. A. Improved Synthesis of Aligned Arrays of Single-Walled Carbon Nanotubes and Their Implementation in Thin Film Type Transistors. *J. Phys. Chem. C* **2007**, *111*, 17879-17886.
13. Kang, S. J.; Kocabas, C.; Ozel, T.; Shim, M.; Pimparkar, N.; Alam, M. A.; Rotkin, S. V.; Rogers, J. A. High-Performance Electronics Using Dense, Perfectly Aligned Arrays of Single-Walled Carbon Nanotubes. *Nat. Nanotechnol.* **2007**, *2*, 230-236.
14. Ding, L.; Yuan, D.; Liu, J. Growth of High-Density Parallel Arrays of Long Single-Walled Carbon Nanotubes on Quartz Substrates. *J. Am. Chem. Soc.* **2008**, *130*, 5428-5429.
15. Rutkowska, A.; Walker, D.; Gorfman, S.; Thomas, P. A.; Macpherson, J. V. Horizontal Alignment of Chemical Vapor-Deposited SWNTs on Single-Crystal Quartz Surfaces: Further Evidence for Epitaxial Alignment. *J. Phys. Chem. C* **2009**, *113*, 17087-17096.
16. Xiao, J.; Dunham, S.; Liu, P.; Zhang, Y.; Kocabas, C.; Moh, L.; Huang, Y.; Hwang, K. C.; Lu, C.; Huang, W.; Rogers, J. A. Alignment Controlled Growth of Single-Walled Carbon Nanotubes on Quartz Substrates. *Nano Lett.* **2009**, *9*, 4311-4319.
17. Maruyama, S.; Kojima, R.; Miyauchi, Y.; Chiashi, S.; Kohno, M. Low-Temperature Synthesis of High-Purity Single-Walled Carbon Nanotubes from Alcohol. *Chem. Phys. Lett.* **2002**, *360*, 229-234.
18. Iwasaki, F.; Iwasaki, H.; Okabe, Y. Growth Rate Anisotropy of Synthetic Quartz Grown in Na<sub>2</sub>CO<sub>3</sub> Solution. *J. Cryst. Growth* **1997**, *178*, 648-652.
19. Jorio, A.; Saito, R.; Hafner, J. H.; Lieber, C. M.; Hunter, M.; McClure, T.; Dresselhaus, G.; Dresselhaus, M. S. Structural (*n*, *m*) Determination of Isolated Single-Wall Carbon Nanotubes by Resonant Raman Scattering. *Phys. Rev. Lett.* **2001**, *86*, 1118-1121.
20. Hedlund, C.; Lindberg, U.; Bucht, U.; Söderkvist, J. Anisotropic Etching of Z-Cut Quartz. *J. Micromech. Microeng.* **1993**, *3*, 65-73.

21. Lakshtanov, D. L.; Sinogeikin, S. V.; Bass, J. D. High-Temperature Phase Transitions and Elasticity of Silica Polymorphs. *Phys. Chem. Minerals* **2007**, *34*, 11-22.
22. Ago, H.; Uehara, N.; Ikeda, K.; Ohdo, R.; Nakamura, K.; Tsuji, M. Synthesis of Horizontally-Aligned Single-Walled Carbon Nanotubes with Controllable Density on Sapphire Surface and Polarized Raman Spectroscopy. *Chem. Phys. Lett.* **2006**, *421*, 399-403.
23. Nguyen, T. T. T.; Bonamy, D.; Van, L. P.; Barbier, L. Cousty, Coarsening of Two-Dimensional Al<sub>2</sub>O<sub>3</sub> Islands on Vicinal (1,-1,0,2) Sapphire Surfaces during Annealing in Air. *Surf. Sci.* **2008**, *602*, 3232-3238.
24. Chokan, T.; Uetake, T.; Yamada, K.; Chiashi, S.; Homma, Y. Effect of Surface Structure of Sapphire A-Face on Directional Carbon Nanotube Growth. *e-J. Surf. Sci. Nanotechnol.* **2009**, *7*, 904-907.

## SYNOPSIS TOC

